Orbital pacing and ocean circulation-induced collapses of the Mesoamerican monsoon over the past 22,000 y

Matthew S. Lachniet[a,1], Yemane Asmerom[b], Juan Pablo Bernal[c], Victor J. Polyak[b], and Lorenzo Vazquez-Selem[d]

[a]Department of Geoscience, University of Nevada, Las Vegas, NV 89154; [b]Department of Earth and Planetary Science, University of New Mexico, Albuquerque, NM 87131; [c]Centro de Geociencias, Universidad Nacional Autónoma de México, Querétaro 76230, Mexico; and [d]Instituto de Geografía, Universidad Nacional Autónoma de México, Coyoacán, Mexico City 04510, Mexico

Edited by James P. Kennett, University of California, Santa Barbara, CA, and approved April 19, 2013 (received for review January 2, 2013)

The dominant controls on global paleomonsoon strength include summer insolation driven by precession cycles, ocean circulation through its influence on atmospheric circulation, and sea-surface temperatures. However, few records from the summer North American Monsoon system are available to test for a synchronous response with other global monsoons to shared forcings. In particular, the monsoon response to widespread atmospheric reorganizations associated with disruptions of the Atlantic Meridional Overturning Circulation (AMOC) during the deglacial period remains unconstrained. Here, we present a high-resolution and radiometrically dated monsoon rainfall reconstruction over the past 22,000 y from speleothems of tropical southwestern Mexico. The data document an active Last Glacial Maximum (18–24 cal ka B.P.) monsoon with similar $\delta^{18}O$ values to the modern, and that the monsoon collapsed during periods of weakened AMOC during Heinrich stadial 1 (*ca*. 17 ka) and the Younger Dryas (12.9–11.5 ka). The Holocene was marked by a trend to a weaker monsoon that was paced by orbital insolation. We conclude that the Mesoamerican monsoon responded in concert with other global monsoon regions, and that monsoon strength was driven by variations in the strength and latitudinal position of the Intertropical Convergence Zone, which was forced by AMOC variations in the North Atlantic Ocean. The surprising observation of an active Last Glacial Maximum monsoon is attributed to an active but shallow AMOC and proximity to the Intertropical Convergence Zone. The emergence of agriculture in southwestern Mexico was likely only possible after monsoon strengthening in the Early Holocene at *ca*. 11 ka.

stalagmite | paleoclimatology | plant domestication | cave | Sierra Madre del Sur

The North American Monsoon (NAM) dominates the summer moisture budget for most of Mexico and the southwestern United States, but despite its proximity to the Atlantic Meridional Overturning Circulation (AMOC) center of action in the North Atlantic Ocean, it remains one of Earth's least understood monsoons because of a lack of high-resolution summer-sensitive proxy records. In particular, the paleoclimatic history of the tropical sector (south of 20°N) of the NAM, which we informally term the Mesoamerican monsoon because of its distinction from the more northerly "core" sector (1) and its links to the broader cultural area (*SI Text*) remains poorly known due to conflicting interpretations of lacustrine proxy data (2). However, common forcings on the global paleomonsoon (3) suggest that the Mesoamerican monsoon should be sensitive to both precessional-scale orbital forcing and ocean circulation variations via changes in the latitudinal position of the Intertropical Convergence Zone (ITCZ) (3). Reconstructions of the East Asian Monsoon (EAM) and South American Summer Monsoon (SASM) from radiometrically dated speleothems (cave calcites) (3–5) showed that monsoon strength was paced by changes in orbital insolation at ~21,000-y orbital precession time scales, and exhibited millennial-scale climate variability linked by atmospheric teleconnections to the North Atlantic region (6–8). Weakest EAM intervals coincided with cold Heinrich events when ocean circulation was disrupted by freshwater forcing into the North Atlantic, whereas the SASM intensity strengthened during stadials, suggesting a hemispheric antiphasing in tropical rainfall linked to migrations in the latitude of the ITCZ. However, the relative orbital and ocean circulation influence on the Mesoamerican monsoon is unconstrained, limiting our ability to test hypotheses of monsoon forcing (3), the peopling of the Americas (9), the Holocene domestication of maize and squash in Mexico (10), climate's influence on past civilizations (11), and to forecast future monsoon variations in an anthropogenically altered climate (12).

Results

Our 22-ka monsoon reconstruction (Fig. 1) is a well-dated and high-resolution paleorainfall record of the Mesoamerican monsoon, and is based on 2,230 stable oxygen isotope ($\delta^{18}O$) values and 50 U-series dates (see *SI Text* for methods; Figs. S1 and S2; Table S1). The Juxtlahuaca Cave stalagmites presented here were recovered ~750 m from the entrance (927 m), in the Sierra Madre del Sur of southwestern Mexico. Juxtlahuaca Cave presents an ideal cave climate with constant temperature (24.2 °C) and constant 100% relative humidity (11, 13, 14). To facilitate comparison of monsoon strength for different time intervals, the speleothem $\delta^{18}O$ records were corrected for changes in the $\delta^{18}O$ of the ocean, which is the moisture source for rainfall in southwestern Mexico and other global monsoon regions (*SI Text*). The effect of this $\delta^{18}O$ sea water correction is to make $\delta^{18}O$ values ~1‰ more negative during the Last Glacial Maximum (LGM), when ice volume was maximal, and with a negligible correction for today. Further, to test for links between Mesoamerican rainfall and hemispheric forcings, we compared our reconstruction (Fig. 1) with the $^{231}Pa/^{230}Th$ ratio in subtropical North Atlantic sediments (15), a proxy for AMOC intensity (*SI Text*), Greenland Ice Sheet $\delta^{18}O$, a proxy for temperature and atmospheric circulation (6), ice volume (16), and sea-surface temperature in the tropical North Atlantic Ocean (17) to show the sequence of deglacial climate events that typify North Atlantic paleoclimatic change (Fig. 1).

Over the past 22 ky Mexico speleothem $\delta^{18}O$ values are marked by intermediate values of −8 to −9‰ Vienna PeeDee Belemnite (VPDB) during both the last 2 ky and the LGM. In contrast, high $\delta^{18}O$ values (−6.3‰) characterize Heinrich stadial 1 (HS1) and the Younger Dryas (YD) intervals (Fig. 1). Low

Author contributions: M.S.L. and J.P.B. designed research; M.S.L., Y.A., J.P.B., and V.J.P. performed research; Y.A. and V.J.P. contributed new reagents/analytic tools; M.S.L., Y.A., J.P.B., V.J.P., and L.V.-S. analyzed data; and M.S.L., Y.A., J.P.B., V.J.P., and L.V.-S. wrote the paper.

The authors declare no conflict of interest.

This article is a PNAS Direct Submission.

Data deposition: The speleothem $\delta^{18}O$ data reported in this paper have been deposited at the National Climatic Data Center, National Oceanic Atmospheric Administration Paleoclimatology Web site, www.ncdc.noaa.gov/paleo/paleo.html.

[1]To whom correspondence should be addressed. E-mail: matthew.lachniet@unlv.edu.

This article contains supporting information online at www.pnas.org/lookup/suppl/doi:10.1073/pnas.1222804110/-/DCSupplemental.

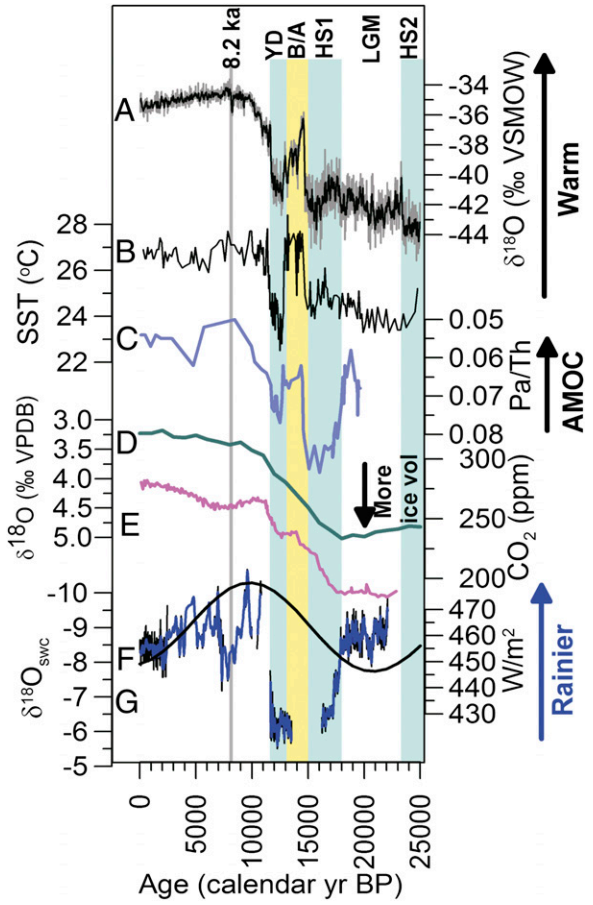

Fig. 1. Comparison of Mesoamerican monsoon strength to proxies for paleoclimatic change in the North Atlantic Ocean. (*A*) North Greenland Ice Sheet Project (NGRIP) $\delta^{18}O$ values on the Greenland Ice Core Chronology 2005 (GICC05) (6). (*B*) SST from Mg/Ca ratios in the Cariaco Basin, Venezuela (17). (*C*) $^{231}Pa/^{230}Th$ ratio, a proxy for AMOC (15). (*D*) LR04 marine benthic foraminifera $\delta^{18}O$ stack (16), a proxy for global ice volume. (*E*) CO_2 record from Antarctica (21). (*F*) Mexico stalagmite $\delta^{18}O$ values from Juxtlahuaca and del Diablo Caves (this study and refs. 11, 14) corrected for changes in the $\delta^{18}O$ of the ocean (*SI Text*) and fitted (bold lines) with 5- and 11-pt running averages (JX-6). (*G*) Summer insolation average (June/July/August, JJA) for 20°N. Vertical bars indicate durations of the 8.2 event, YD, B/A, HS1 and 2, the LGM.

$\delta^{18}O$ values are evident in the Early Holocene at *ca*. 9.5 ka, after which time a Holocene-long $\delta^{18}O$ increase is interrupted by several centennial- to millennial-scale shifts to higher values, most notably between *ca*. 7 and 9 ka. Today, the $\delta^{18}O$ value of rainfall in the Mesoamerican monsoon is strongly controlled by the amount effect (11, 18), whereby intense convection results in low $\delta^{18}O$ values and vice versa, and these rainwater $\delta^{18}O$ variations are recorded in stalagmite $\delta^{18}O$ variations after filtering through the epikarst (13). We conclude that the modern and LGM monsoon states were of approximately equal strengths and that the monsoon abruptly collapsed during early HS1 beginning at 18 ka. Although our stalagmite contains a hiatus during the Bølling/Allerød (B/A), perhaps due to drip rerouting above stalagmite JX-2, the record from Lake Petén Itzá (19) suggests moist conditions and a strong Mesoamerican monsoon. The monsoon was weak during the YD between 12.9 and 11.6 ka, after which time it strengthened at the YD/Early Holocene boundary. Considered on orbital time scales, the Mesoamerican monsoon strength today and at the LGM is of intermediate strength, was strongest during periods of the Early Holocene (lowest $\delta^{18}O$ values), and weakest during the deglacial cold episodes HS1 and the YD (highest $\delta^{18}O$ values). We refer to these three monsoon states as "active," "strong," and "weak," respectively.

Discussion

Forcing of the LGM Mesoamerican Monsoon. The observation of similar modern and LGM Mesoamerican monsoon strength is a surprising result because of the lower specific humidity associated with cooler temperatures, such as is indicated by 3–4 °C sea-surface temperature (SST) depression relative to modern in the Cariaco Basin (17) and lower land-surface temperatures (LST) on the Yucatan Peninsula (20). Thus, the low LGM $\delta^{18}O$ values may be explained by a similar degree of air-mass rainout as today. The stalagmite $\delta^{18}O$ values also contain a temperature imprint: a decrease in LST of ~3–4 °C is responsible for making the stalagmite $\delta^{18}O$ values higher by ~0.6–0.8‰ due to the water–carbonate precipitation temperature (13), leading to apparently slightly weaker monsoons during cold periods. However, this influence on the stalagmite $\delta^{18}O$ profile (+0.6 to +0.8‰) is small relative to the observed magnitude of $\delta^{18}O$ changes related to monsoon strength (*ca*. 3–4‰), and it would have been offset by the decrease in $\delta^{18}O$ values of precipitation during cold periods due to the atmospheric temperature effect. Because our observations contradict a simple thermodynamic forcing of monsoon strength via atmospheric water vapor content, an alternative mechanism for maintaining an active LGM monsoon must be considered.

A key similarity between today and the LGM is that local summer insolation at 20°N reached precessional-scale minima, and we suggest that the similar monsoon strength was forced by nearly equal summer insolation despite the high ice volume, lower temperature, and lower CO_2 (21) boundary conditions at the LGM (Fig. 1). Today, monsoon strength is positively correlated both with the magnitude of the ocean-to-land temperature gradient ($\Delta T_{SST\text{-}LST}$) and proximity to the ITCZ, and we hypothesize that similar processes affected the Mesoamerican monsoon during the LGM in response to similar orbital forcing. However, insolation forcing is unlikely to be the only driver on monsoon strength during deglaciation, because weak monsoon intervals during the YD and HS1 also occurred at times of higher summer insolation and low temperatures.

Atlantic Ocean Circulation and ITCZ Forcing of the Mesoamerican Monsoon. An alternative hypothesis to explain the similar LGM and modern monsoon strength, potentially acting in concert with insolation forcing, is via the latitudinal position of the ITCZ. Today, the ITCZ migrates seasonally in response to the warmest SSTs, reaching its northern most extent ~10–12°N in late boreal summer over the eastern Pacific warm pool (22) off southwestern Mexico. On millennial time scales, the ITCZ latitudinal position has been shown to be forced by the strength of the ocean circulation (AMOC) (23), so we compared our record to the ocean circulation $^{231}Pa/^{230}Th$ proxy in the North Atlantic ocean. Our Mesoamerican monsoon reconstruction shares several features with the $^{231}Pa/^{230}Th$ AMOC proxy, including intermediate AMOC during the LGM, a pronounced weakening during HS1, and an Early Holocene increase. Because our record displays key similarities to the $^{231}Pa/^{230}Th$ record, we suggest that Mesoamerican monsoon strength is also related to the vigor of the AMOC and its consequent influence on the latitude and strength of the ITCZ. Active AMOC maintains high SST in the North Atlantic as a result of cross-equatorial northward transport of warm surface waters, which in turn favors a northerly location of the ITCZ, and vice versa.

To further test the hypothesis of an ITCZ position influence on the Mesoamerican monsoon, we compared our record to other hydrologic proxy records in the global monsoon regions temporally (Fig. 2) and spatially (Fig. S3) to AMOC variations

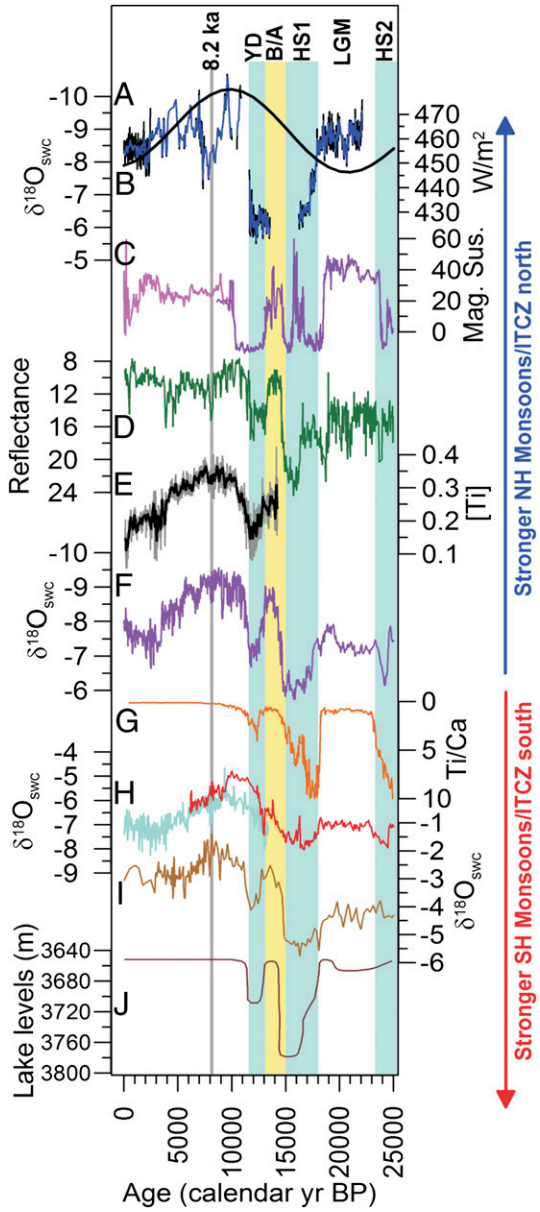

Fig. 2. Hydrological proxies for the North and South American monsoon regions show antiphased behavior. (*A*) Mexico stalagmite $\delta^{18}O$ reconstruction of the Mesoamerican monsoon. (*B*) Summer insolation average (JJA) for 20°N. (*C*) Lake Petén Itzá magnetic susceptibility record on the original chronology (light blue) for the Holocene (19) and an updated (blue) chronology for the Late Glacial Period (24). (*D*) Reflectance in Cariaco Basin sediment cores (26). (*E*) Ti concentrations in Cariaco Basin sediment (32). (*F*) Asian Monsoon proxy reconstruction from Dongge and Hulu Caves (3). (*F*) Ti concentrations in Cariaco basin sediments, positively correlated with greater continental runoff (32). (*G*) Ti/Ca ratio in northeastern Brazil margin sediments, a proxy for continental runoff (28). (*H*) Western Amazon stalagmite monsoon reconstructions from Santiago (orange) and Tigre Perdido Caves (light green) (8, 27). (*I*) Stalagmite monsoon reconstruction from Botuverá Cave, southern Brazil (4). (*J*) Lake level reconstructions for the Bolivian altiplano (31). Stalagmite $\delta^{18}O$ records have been adjusted for the change in $\delta^{18}O$ values of the ocean, denoted with the subscript "swc." The *y* axis for the South American monsoon records are reversed for better comparison with northern Hemisphere records.

for the Early Holocene, YD, HS1, and LGM time slices. The records exhibit a strong similarity in character, with pronounced hydrologic anomalies during the LGM, deglacial, and Holocene time periods that are antiphased between the hemispheres, as would be predicted by an ITCZ control on monsoon strength. Prominently, active monsoon conditions during the LGM are apparent in the Mexico speleothem reconstruction and in high magnetic susceptibility measurements in Lake Petén Itzá in Guatemala (19, 24), and in similar Early Holocene and LGM (*ca*. 24 ka) Central American monsoon strength (25), demonstrating wetness on both the Atlantic and Pacific coasts of Mesoamerica and Central America. Based on these observations, we conclude that the active LGM monsoon was aided by a proximal location of the ITCZ to the Mexican landmass, which facilitated moisture delivery into the monsoon system. This mechanism is consistent with modern climate dynamics, such as cooling similar to a modern La Niña event (Fig. S4), which results in increased $\Delta T_{SST\text{-}LST}$, a more northerly position of the ITCZ (1), and low $\delta^{18}O$ values (18) associated with the monsoon.

Continental river runoff in the Cariaco Basin of northern South America (26) shows intermediate levels during the LGM, indicating that the monsoon was somewhat weaker than today, although interpretation of the LGM-to-modern change in this record is complicated by the influence of deglacial sea-level rise on ocean circulation. The Mesoamerican monsoon data are similar to observations of the EAM (3), which shows similar seawater–corrected $\delta^{18}O$ values during the LGM as today, a likely response to the common forcing of summer insolation. Similarly, speleothem $\delta^{18}O$ records from South America [Botuverá (4) and Santiago and Tigre Perdido (8, 27) Caves] indicate similar to somewhat stronger monsoon strength at the LGM relative to today, but continental runoff in northeastern Brazil appears to have been low (28).

Following an active LGM monsoon, the Mesoamerican monsoon collapsed abruptly at the onset of HS1 (18 ka) and remained weak for at least 700 y. General Circulation Model (GCM) results indicate an AMOC slowdown during freshwater release into the North Atlantic during Heinrich events, which provokes a southward displacement of the ITCZ (29). A southward displaced ITCZ during HS1 is supported by observations of minimum Ti concentrations in the Cariaco Basin (26), increased wetness in northeast Brazil (28), expansion of paleolakes and glaciers on the Bolivian altiplano (30, 31), and a weak EAM (3) (Fig. S3). The Mesoamerican monsoon was also weak during the YD (6) in southwestern Mexico, Lake Petén Itzá (low magnetic susceptibility), and in the Cariaco Basin (low Ti concentrations) (32) when SST was depressed by 3–4 °C (17). AMOC was weakened during the YD relative to interstadial conditions (15). In contrast, locally wet conditions mark the YD in South America (Fig. 2), but to a lesser extent than during HS1. The ITCZ was thus apparently weaker and displaced to the south during the YD (Fig. S3).

A strengthening of the Mesoamerican monsoon coincided with the YD/Early Holocene transition in Greenland (6), and was associated with a peak in summer insolation associated with the precession cycle at *ca*. 9.5 ka. Subsequently the monsoon gradually weakened during the Holocene, and was punctuated by a weak monsoon interval between 9.3 and 7.4 ka spanning the 8.2-ka event (14). The Holocene monsoon weakening supports the hypothesis of an orbital pacing (3, 33) of the Mesoamerican monsoon, whereby decreasing summer insolation at 20°N resulted in a southward displacement of the ITCZ. Similar trends are also evident in decreasing Holocene wetness in the Cariaco Basin, the EAM, and a monsoon strengthening in South America.

Regional Records of the Mesoamerican Monsoon. A synthesis of Mesoamerican climate records (Fig. 3), including a well-dated central Mexico glacial chronology (34) and lacustrine records from the Yucatan Peninsula (19, 35) and Central Mexico (36–38), shows that paleoclimate varied coherently since the LGM (all records are shown on a calendar age scale; see *SI Text* for methods). Our observation of an active LGM monsoon is supported by wet conditions inferred from high magnetic susceptibility in Lake

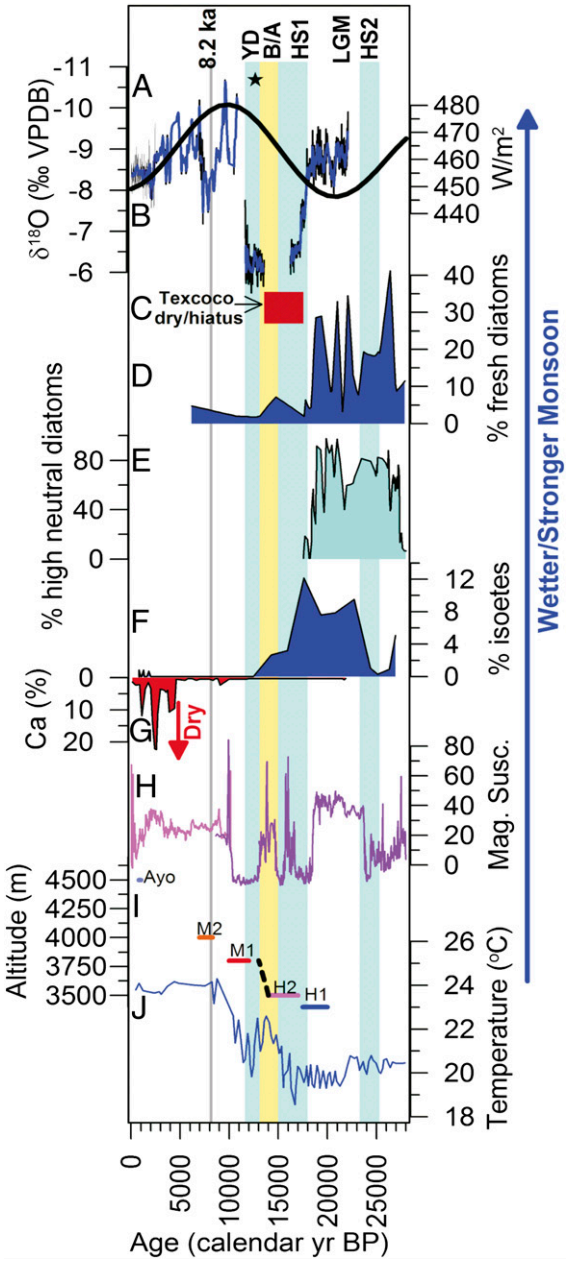

Fig. 3. Comparison of Mesoamerica paleoclimate records shows a coherent monsoon response and a wet LGM. (*A*) Mexico stalagmite $\delta^{18}O$ monsoon record. (*B*) JJA mean insolation for 20°N latitude. (*C*) Interval of sedimentary hiatus on west shore of L. Texcoco. (*D*) Sum of open-water diatoms in main basin of L. Texcoco (38). (*E*) Percentage of high neutral diatoms in L. Chalco, southern Basin of Mexico (39). (*F*) Percentage of *isoetes* spores in L. Pátzcuaro sediments. (*G*) Percent Ca, a proxy for marl precipitation during dry conditions (36). (*H*) Lake Petén Itzá magnetic susceptibility record (19). (*I*) Glaciation altitudinal limits on Iztaccíhautl (34). (*J*) Pollen-inferred land surface temperatures on the Yucatan Peninsula (35); black star is the age of the earliest securely dated human remains in Mexico (49), dating to the YD.

Petén Itzá sediments (19), during which time pollen-inferred LSTs were lowered by ∼4 °C (35). Maximum glacial extent in highland Mexico between *ca*. 21 and 17.5 ka (34) (Hueyatlaco-1 advance) coincided with a high Lake Chalco level (37) and a high abundances of *isoetes* spores (an aquatic fern of oligotrophic lakes) in Lake Pátzcuaro in the western Mexican highlands (36). High abundances of open water (38) and high neutral diatoms (pH ∼7; medium to low electrical conductivity) (39) indicate fresh lakes in the Basin of Mexico. The available evidence supports a wet and cold LGM in Mesoamerica, although the radiometric control of the central Mexico lake chronologies is poor (*SI Text*). The wet conditions inferred from the lake records suggest that the LGM monsoon was similar in effective strength relative to today, despite the lower specific humidity associated with decreased atmospheric temperatures during cold periods.

Widespread evidence for dry conditions in Mesoamerica documents a coherent Mesoamerican monsoon collapse at the LGM to HS1 transition and during the YD (Fig. 3). Gypsum deposition in Lake Petén Itzá was attributed to evaporative conditions and low lake levels (19) during Heinrich stadials and the YD, when LSTs were similar to the LGM (35). In the Mexican highlands, a decrease in circumneutral (pH ∼7) diatom abundance in Lake Chalco sediments (37) is evident during HS1, and glaciers retreated upslope. These observations suggest that moisture was a limiting factor in glacier mass balance during HS1, a contention supported by low levels of Lake Chalco between 18.5 and 14.5 ka (37) and a sedimentary hiatus on the margins of ancient Lake Texcoco (38). Post-YD monsoon strengthening is indicated by low stalagmite $\delta^{18}O$ values, lake filling in southwestern Mexico at 10.85 ka (40), and establishment of a mesic Yucatan forest by 11.25 ka (19). An abrupt Early Holocene monsoon weakening between 7.5 and 9.0 ka was associated with the only major Holocene glaciation on Iztaccíhuatl, (Milpulco-2) (34). A Late Holocene drying trend is evident in higher stalagmite $\delta^{18}O$ values by *ca*. 3.5 ka and increased marl precipitation in Lago Pátzcuaro in western Mexico (36).

Mesoamerican and Global Paleomonsoons. Based on a comparison of our monsoon reconstruction to orbital forcing, SST, and AMOC variations, we conclude that the Mesoamerican monsoon responded similarly to the shared global forcings evident in the paleomonsoon responses in Asia and South America (3, 33) over the last 22 ka (Fig. S3). Based on correlations to paleoclimate proxy records, we conclude that the primary controls on Mesoamerican monsoon strength were (*i*) local summer insolation values driven by the precession cycle, and (*ii*) the AMOC-controlled position of the ITCZ. The conclusion that AMOC was active during the LGM is supported by the low $^{231}Pa/^{230}Th$ ratios in the North Atlantic Ocean, and detailed observations of $^{231}Pa/^{230}Th$ ratio in Atlantic Ocean sediments that document a shallower deepwater overturning cell, but with a rate of AMOC similar or greater in strength than today (41). The paleoceanographic data thus document an active AMOC during the LGM, favorable for forcing an active LGM Mesoamerican monsoon via a northerly position of the ITCZ. GCM results also support our conclusions of an active LGM monsoon. In a combined modern and LGM run of the community climate model (CCM3) (42), wet summer conditions in southwestern Mexico southward to 20°N are simulated for the LGM, and we show that a strong monsoon extended to at least 17.4°N. Conversely, freshwater "hosing" model experiments, where a large volume of freshwater is added to the North Atlantic Ocean to simulate meltwater discharge during Heinrich stadials, result in a southward displacement of the ITCZ (23, 29). The model experiments are consistent with increased $^{231}Pa/^{230}Th$ ratios in the North Atlantic Ocean during HS1 and the YD (15), recording a weakening of the AMOC and a southward displacement of the ITCZ. The tropical hydrologic response appears to be strongest and most coherent during HS1, with clear evidence for a southward displacement of the ITCZ, with a weaker response in the YD and Early Holocene (Fig. S3).

Our monsoon reconstruction differs in important characteristics from the East Asian and South American monsoons (Fig. 2). Most prominently, monsoon collapses during HS1 and the YD were of apparently equal magnitude in Mesoamerica, whereas the EAM displays a weaker YD response relative to HS1 which is more similar to the AMOC forcing. There is a less consistent hydrological

response in the SASM during the YD, with the expansion of altiplano lakes, increased runoff to the Brazil margin, and lower $\delta^{18}O$ in the Botuverá stalagmite recording a stronger monsoon (28, 31, 43, 44), yet stalagmites in the western Amazon and Amazon river runoff indicating a weaker monsoon (8, 45). Part of this discrepancy is likely due to the presence of a precipitation dipole over the western Amazon and northeast Brazil, where there is an opposite rainfall response to climate events during the Late Glacial (44, 46). For example, the YD was somewhat wetter than today in northeast and southern Brazil, but in the western Amazon was marked by a transition from wet to dry conditions (8, 27, 44). We also observe enhanced Holocene $\delta^{18}O$ anomalies and hence rainfall variability in Mesoamerica relative to Asia and South America. These observations suggest that the abrupt transitions and amplified isotopic variability in the Mesoamerican monsoon may be a result of its proximal location to the AMOC center of action in the North Atlantic Ocean, possibly enhanced by a high sensitivity or a threshold response of monsoon strength to ITCZ position.

Implications for Mesoamerican Monsoon Forcing and Emergence of Agriculture. Our conclusion of an active LGM summer monsoon similar to today differs from prior interpretations of wetness in central and southwestern Mexico. Previous workers suggested that such wetness was derived from winter extratropical air masses guided by a southward-displaced jet stream (20, 36) and/or polar outbreaks (*nortes*) (19). If the extratropical moisture hypothesis is correct, then winter precipitation would have been maximal during periods associated with the most extreme southward displacement of the ITCZ during the YD and HS1 when AMOC was slow. To test this prediction, we analyzed isotopic data for Chihuahua in northern Mexico (28.63°N, 106.07°W), which receives both summer and winter rainfall. Because winter precipitation $\delta^{18}O$ values [$-9.2 \pm 2.9\%$ Vienna standard mean ocean water (VSMOW)] are about 3% lower than summer ($-6.2 \pm 3.3\%$ VSMOW), the winter precipitation hypothesis would predict that stalagmite $\delta^{18}O$ values would have decreased by several permil during the YD and HS1. In fact, we see the opposite: $\delta^{18}O$ values increased during these times. Further, the winter rainfall hypothesis suffers from other weaknesses. Today, rainfall is dominated by the summer monsoon, with winter rainfall providing less than 4% to annual totals to southwestern Mexico because of low specific humidity in winter air masses (Figs. S5–S7). Further, neither enhanced winter westerlies nor polar outbreaks alone can account for observed regional wetness in Mesoamerica (Fig. 2), because orographic effects today limit winter precipitation to windward slopes (Fig. S8). This contrasts with widespread monsoon wetness observed both today and during the LGM. A drastic shift in the latitude of the westerlies deep into the tropics is also difficult to reconcile with modern and Late Glacial climate dynamics and requires a no-modern-analog climate state. GCM output indicates the zone of maximum winter westerly precipitation over North America at the LGM was restricted to *ca*. 30 and 40°N (42), and it is difficult to envision the presence of pluvial lakes at these latitudes (47) if the winter rainfall band was displaced to 17°N latitude.

Our monsoon reconstruction has implications for Mesoamerican plant domestication, because agricultural emergence after human colonization was hypothesized to have been impossible during the Late Glacial Period because of low CO_2, low temperatures, and aridity (48). Although our data support an active monsoon during the LGM (18–22 ka), the earliest securely dated human remains in Mexico significantly postdate the LGM to 12,650 ± 70 calendar y B.P. (10,755 ± 75 ^{14}C y B.P.) (49), coinciding with the YD weak monsoon interval (Fig. 1). However, the presence of the earliest known pre-Clovis artifacts in North America, dated to as early as 15.5 ka, and their arrival in South America (Monte Verde site) by *ca*. 14.5 ka (50, 51), suggests that humans may have also been present in Mesoamerica during the B/A interstadial, when the Mesoamerican monsoon was strong (19), and CO_2 concentrations of ca. 240 ppm approached Early Holocene concentrations (*ca*. 260 ppm). In contrast, had humans traversed Mesoamerica during HS1 between 17.0 and 14.5 ka, they would have encountered a weak monsoon when CO_2 was <220 ppm. Neither HS1 nor the YD appears to present suitable monsoon conditions to support agriculture, and no solid evidence of human occupation of Mesoamerica during the wet LGM is available. Further, the absence of evidence for agricultural emergence during the B/A may be related to the relatively short duration of suitable climatic conditions, absence of a significant human population, or other factors. Thus, our data most strongly support the hypothesis that agriculture in Mesoamerica was first possible when a strong monsoon coincided with climate warming and high atmospheric CO_2 concentrations *ca*. 11 ka.

Our data can further constrain the climatic conditions associated with maize domestication, likely from a wild teosinte (*Zea Mays* ssp. *parviglumis*; hereafter "teosinte") ancestor in the Balsas River Basin by ~9.0 ka (10, 52). Maize was likely cultivated with squash at lake margins sometime during the earlier half of the interval between 10.0 and 5.0 ka (40), and archeological evidence documents the presence of maize starch on grinding tools by *ca*. 8.7 ka in the Balsas River drainage (52). Our data, including the Holocene section from Cueva del Diablo, located near the town of Teloloapan where a modern stand of teosinte is present (40), suggests that the Early Holocene was marked by highly variable rainfall, from very wet at 9.6 ka, to the most pronounced Holocene dry period between 9.0 and 7.2 ka, and a return to wetter climate between 7.0 and 4.0 ka. The occurrence of maize and squash phytoliths suggests that lake margin agriculture may have been used to exploit the high water tables in this environment as an adaptation to the vagaries of an unstable Holocene climate.

Materials and Methods

We analyzed four stalagmites from southwestern Mexico for oxygen-stable isotopes ($\delta^{18}O$) and U-series ratios (Figs. S1 and S2). The Juxtlahuaca Cave stalagmites were dated at the University of New Mexico radiogenic isotope laboratory on a Thermo Neptune multicollector inductively coupled plasma mass spectrometer. Subsample powders of ~50–200 mg were dissolved in nitric acid and mixed with a ^{229}Th–^{233}U–^{236}U spike. Analytical uncertainties are 2σ of the mean, and include analytical errors and uncertainty in the initial $^{230}Th/^{232}Th$ ratios, which was set to 4.4 ppm (assuming a bulk earth $^{232}Th/^{238}U$ value of 3.8). Our monsoon reconstruction is based on 2,230 $\delta^{18}O$ analyses conducted at the Las Vegas Isotope Science Laboratory at the University of Nevada, Las Vegas (LVIS: samples JX-2, -6, and -10), and the Universidad Autónoma de Mexico (CBD-2) for $\delta^{18}O$ and $\delta^{13}C$, mostly at a 0.5- or 1.0-mm sampling interval, corresponding to a temporal resolution of ~2 y for the last 2 ka, 10–12 y for the LGM, HS1, and YD, and ~60 y for the Holocene. The $\delta^{18}O$ values measured at LVIS were determined with a Kiel IV automated carbonate preparation device whereby samples were reacted at 70 °C with phosphoric acid. The CO_2 gas was separated and purified using cryogenic trapping, and analyzed on a ThermoElectron Delta V Plus stable isotope ratio mass spectrometer in dual inlet mode. $\delta^{18}O$ values were corrected with an internal standard (USC-1) whose value was determined by comparison with the international standards NBS-18 and NBS-19. Long-term internal precision of USC-1, NBS-18, and NBS-19 is better than 0.1% $\delta^{18}O$. All $\delta^{18}O$ values are expressed in standard δ-% notation in deviations relative to the VPDB scale.

ACKNOWLEDGMENTS. We thank Prof. Andrés Ortega Jiménez, Juxtlahuaca Cave docent, for collaboration. We also thank Francisco Navarrete and German Hernández Becerra (Comisión Federal de Electricidad of Mexico) for providing long-term data from the Colotlipa weather station. This paper also benefitted from the valuable comments of two anonymous reviewers and an insightful review from the editor. Research was supported by the National Science Foundation (NSF) Paleoperspectives on Climate Change (Grant ATM-1003558) and the Major Research Instrumentation program of the Earth Science Division of NSF (EAR/MRI) (Grant EAR-0521196) programs, the National Geographic Society (Grant 8828-10), Consejo Nacional de Ciencia y Technología (Mexico) (Grants 44016 and 77018) and Universidad Autónoma de Mexico's Programa de Apoyo a Proyectos de Investigación e Innovación Tecnológica Grants IN116906 and IN112008.

1. Liebmann B, et al. (2008) characteristics of North American monsoon summertime rainfall with emphasis on the Monsoon. *J Clim* 21:1277–1294.
2. Metcalfe S, O'Hara SL, Caballero M, Davies S (2000) Records of Late Pleistocene-Holocene climatic change in Mexico - a review. *Quat Sci Rev* 19:699–721.
3. Cheng H, Sinha A, Wang X, Cruz FW, Edwards RL (2012) The Global Paleomonsoon as seen through speleothem records from Asia and the Americas. *Clim Dyn* 39: 1045–1062.
4. Cruz FW, Jr., et al. (2005) Insolation-driven changes in atmospheric circulation over the past 116,000 years in subtropical Brazil. *Nature* 434(7029):63–66.
5. Wang YJ, et al. (2001) A high-resolution absolute-dated late Pleistocene Monsoon record from Hulu Cave, China. *Science* 294(5550):2345–2348.
6. Svensson A, et al. (2008) A 60,000 year Greenland stratigraphic ice core chronology. *Clim. Past* 4(1):47–57.
7. Kanner LC, Burns SJ, Cheng H, Edwards RL (2012) High-latitude forcing of the South American summer monsoon during the Last Glacial. *Science* 335(6068):570–573.
8. Mosblech NAS, et al. (2012) North Atlantic forcing of Amazonian precipitation during the last ice age. *Nat Geosci* 5:817–820.
9. Goebel T, Waters MR, O'Rourke DH (2008) The late Pleistocene dispersal of modern humans in the Americas. *Science* 319(5869):1497–1502.
10. Piperno DR, Pearsall DM (1998) *The Origins of Agriculture in the Lowland Neotropics* (Academic, London), pp 400.
11. Lachniet MS, Bernal JP, Asmerom Y, Polyak V, Piperno D (2012) A 2400-yr rainfall history links climate and cultural change in Mexico. *Geology* 40(3):259–262.
12. IPCC (2007) *Climate Change 2007: Synthesis Report. Contribution of Working Groups I, II, and III to the Fourth Assessment Report of the Intergovernmental Panel on Climate Change* [Core Writing Team, eds Pachauri RK, Reisinger A] (IPCC, Geneva, Switzerland), p 104.
13. Lachniet MS (2009) Climatic and environmental controls on speleothem oxygen isotope values. *Quat Sci Rev* 28:412–432.
14. Bernal JP, et al. (2011) A speleothem record of Holocene climate variability from southwestern Mexico. *Quat Res* 75:104–113.
15. McManus JF, Francois R, Gherardi JM, Keigwin LD, Brown-Leger S (2004) Collapse and rapid resumption of Atlantic meridional circulation linked to deglacial climate changes. *Nature* 428(6985):834–837.
16. Lisiecki LE, Raymo ME (2005) A Pliocene-Pleistocene stack of 57 globally distributed benthic $\delta^{18}O$ records. *Paleoceanography* 20(PA1003), 10.1029/2004PA001071.
17. Lea DW, Pak DK, Peterson LC, Hughen KA (2003) Synchroneity of tropical and high-latitude Atlantic temperatures over the last glacial termination. *Science* 301(5638): 1361–1364.
18. Lachniet MS (2009) Sea surface temperature control on the stable isotopic composition of rainfall in Panama. *Geophys Res Lett* 36(L03701) 10.1029/2008GL036625.
19. Hodell DA, et al. (2008) An 85-ka record of climate change in lowland Central America. *Quat Sci Rev* 27(11–12):1152–1165.
20. Correa-Metrio A, Lozano-García S, Xelhuantzi-López S, Nájera-Sosa S, Metcalfe S (2012) Vegetation in western Central Mexico during the last 50,000 years: Modern analogs and climate in the Zacapu Basin. *J Quat Sci* 27(5):509–518.
21. Monnin E, et al. (2001) Atmospheric CO_2 concentrations over the last glacial termination. *Science* 291(5501):112–114.
22. Amador JA, Alfaro EJ, Lizano OG, Magaña VO (2006) Atmospheric forcing of the eastern tropical Pacific: A review. *Prog Oceanogr* 69:101–142.
23. Merkel U, Prange M, Schulz M (2010) ENSO variability and teleconnections during glacial times. *Quat Sci Rev* 29:86–100.
24. Escobar J, et al. (2012) A ~43-ka record of paleoenvironmental change in the Central American lowlands inferred from stable isotopes of lacustrine ostracods. *Quat Sci Rev* 37:92–104.
25. Lachniet MS, et al. (2009) Late Quaternary moisture export across Central America and to Greenland: Evidence for tropical rainfall variability from Costa Rican stalagmites. *Quat Sci Rev* 28:3348–3360.
26. Peterson LC, Haug GH (2006) Variability in the mean latitude of the Atlantic Intertropical Convergence Zone as recorded by riverine input of sediments to the Cariaco Basin (Venezuela). *Palaeogeogr Palaeoclimatol Palaeoecol* 234:97–113.
27. van Breukelen MR, Vonhof HB, Hellstrom JC, Wester WCG, Kroon D (2008) Fossil dripwater in stalagmites reveals Holocene temperature and rainfall variation in Amazonia. *Earth Planet Sci Lett* 275(1–2):54–60.
28. Jaeschke A, Ruhlemann C, Arz H, Heil G, Lohmann G (2007) Coupling of millennial-scale changes in sea surface temperature and precipitation off northeastern Brazil with high-latitude climate shifts during the last glacial period. *Paleoceanography*, 10.1029/2006PA001391.
29. Vellinga M, Wood RA (2002) Global climatic impacts of a collapse of the Atlantic thermohaline circulation. *Clim Change* 54(3):251–267.
30. Blard P-H, et al. (2009) Late local glacial maximum in the Central Altiplano triggered by cold and locally-wet conditions during the paleolake Tauca episode (17-15 ka, Heinrich 1). *Quat Sci Rev* 28:3414–3427.
31. Placzek C, Quade J, Patchett PJ (2006) Geochronology and stratigraphy of late Pleistocene lake cycles on the southern Bolivian Altiplano: Implications for causes of tropical climate change. *Geol Soc Am Bull* 118:515–532.
32. Haug GH, Hughen KA, Sigman DM, Peterson LC, Röhl U (2001) Southward migration of the intertropical convergence zone through the Holocene. *Science* 293(5533): 1304–1308.
33. Kutzbach JE, Liu X, Liu Z, Chen G (2008) Simulation of the evolutionary response of global summer monsoon to orbital forcing over the past 280,000 years. *Clim Dyn* 30: 567–579.
34. Vazquez-Selem L, Heine K (2011) Late Quaternary Glaciation in Mexico. *Quaternary Glaciations - Extent and Chronology, A Closer Look*, eds Ehlers J, Gibbard PL, Hughes PD (Elsevier, Amsterdam), pp 849–861.
35. Correa-Metrio A, et al. (2012) Rapid climate change and no-analog vegetation in lowland Central America during the last 86,000 years. *Quat Sci Rev* 38:63–75.
36. Bradbury JP (2000) Limnologic history of Lago de Patzcuaro, Michoacan, Mexico for the past 48,000 years; impacts of climate and man. *Palaeogeogr Palaeoclimatol Palaeoecol* 163(1–2):69–95.
37. Caballero M, Ortega-Guerrero A (1998) Lake levels since about 40,000 years ago at Lake Chalco, near Mexico City. *Quat Res* 50:69–79.
38. Bradbury JP (1989) Late Quaternary lacustrine paleoenvironments in the Cuenca de Mexico. *Quat Sci Rev* 8:75–100.
39. Caballero-Miranda C (1997) The last glacial maximum in the basin of Mexico: The diatom record between 34,000 and 15,000 years BP from Lake Chalco. *Quat Int* 43/44: 125–136.
40. Piperno DR, et al. (2007) Late Pleistocene and Holocene environmental history of the Iguala Valley, Central Balsas Watershed of Mexico. *Proc Natl Acad Sci USA* 104(29): 11874–11881.
41. Lippold J, et al. (2012) Strength and geometry of the glacial Atlantic Meridional Overturning circulation. *Nat Geosci* 5:813–816.
42. Kim SJ, et al. (2008) High-resolution climate simulation of the last glacial maximum. *Clim Dyn* 31(1):1–16.
43. Baker PA, et al. (2001) Tropical climate changes at millennial and orbital timescales on the Bolivian Altiplano. *Nature* 409(6821):698–701.
44. Cheng H, et al. (2013) Climate change patterns in Amazonia and biodiversity. *Nat Commun* 4:1411.
45. Maslin MA, Burns SJ (2000) Reconstruction of the Amazon Basin effective moisture availability over the past 14,000 years. *Science* 290(5500):2285–2287.
46. Cruz FW, et al. (2009) Orbitally driven east-west antiphasing of South American precipitation. *Nat Geosci* 2(3):210–214.
47. Enzel Y, Wells SG, Lancaster N (2003) Late Pleistocene lakes along the Mojave River, Southeast California. *Spec Pap Geol Soc Am* 368:61–77.
48. Richerson PJ, Boyd R, Bettinger RL (2001) Was agriculture impossible during the Pleistocene but mandatory during the Holocene? A climate change hypothesis. *Am Antiq* 66(3):387–411.
49. Gonzalez S, et al. (2003) Earliest humans in the Americas: New evidence from México. *J Hum Evol* 44(3):379–387.
50. Dillehay TD (2009) Probing deeper into first American studies. *Proc Natl Acad Sci USA* 106(4):971–978.
51. Waters MR, et al. (2011) The Buttermilk Creek complex and the origins of Clovis at the Debra L. Friedkin site, Texas. *Science* 331(6024):1599–1603.
52. Piperno DR, Ranere AJ, Holst I, Iriarte J, Dickau R (2009) Starch grain and phytolith evidence for early ninth millennium B.P. maize from the Central Balsas River Valley, Mexico. *Proc Natl Acad Sci USA* 106(13):5019–5024.